Insect Biochemistry and Molecular Biology 113 (2019) 103211

Contents lists available at ScienceDirect

Insect Biochemistry and Molecular Biology

journal homepage: www.elsevier.com/locate/ibmb

Proteomic analysis of *Laodelphax striatellus* gonads reveals proteins that may manipulate host reproduction by *Wolbachia*

Hai-Jian Huang[1], Jia-Rong Cui[1], Jie Chen, Xiao-Li Bing, Xiao-Yue Hong*

Department of Entomology, Nanjing Agricultural University, Nanjing, Jiangsu 210095, China

ARTICLE INFO

Keywords:
Wolbachia
Laodelphax striatellus
Cytoplasmic incompatibility
Male gonads
Cytosol amino-peptidase-like

ABSTRACT

Wolbachia are intracellular bacteria that manipulate host reproduction by several mechanisms including cytoplasmic incompatibility (CI). However, the underlying mechanisms of *Wolbachia*-induced CI are not entirely clear. Here, we monitored the *Wolbachia* distribution in the male gonads of the small brown planthopper (*Laodelphax striatellus*, SBPH) at different development stages, and investigated the influence of *Wolbachia* on male gonads by a quantitative proteomic analysis. A total of 276 differentially expressed proteins were identified, with the majority of them participating in metabolism, modification, and reproduction. Knocking down the expression of outer dense fiber protein (ODFP) and venom allergen 5-like (VA5L) showed decreased egg reproduction, and these two genes might be responsible for *Wolbachia* improved fecundity in infected *L. striatellus*; whereas knocking down the expression of cytosol amino-peptidase-like (CAL) significantly decreased the egg hatch rate in *Wolbachia*-uninfected *L. striatellus*, but not in the *Wolbachia*-infected one. Considering that the mRNA/protein level of CAL was downregulated by *Wolbachia* infection and ds*CAL* treatment closely mimicked *Wolbachia*-induced CI, we presumed that CAL might be one of the factors determining the CI phenotype.

1. Introduction

Wolbachia are common intracellular bacteria that infect ~40% of arthropod species as well as other invertebrates (Zug and Hammerstein, 2012). These endosymbionts can be vertically transmitted through host eggs and manipulate host reproduction in diverse ways, including male killing, feminization, parthenogenesis, and cytoplasmic incompatibility (CI) (Hilgenboecker et al., 2008). Among these manipulations, CI is the most common effect, in which eggs derived from crosses between *Wolbachia*-infected males and uninfected females fail to develop. However, infected females are able to produce viable progeny regardless of whether they mate with infected or uninfected males through rescue mechanisms (Werren, 1996; Beckmann et al., 2019). CI provides a reproductive advantage to *Wolbachia*-infected females and greatly increases the proportion of *Wolbachia* infected individuals within a population (Hoffmann et al., 1990).

Reproductive manipulation of CI makes *Wolbachia* become an important control agent against harmful arthropods (Xi et al., 2005). However, the molecular mechanisms underlying CI are not entirely clear, yet several evidences indicated that CI occurred at the first mitosis following fertilization, when chromosomes derived from paternal delayed in condensation, but the maternal chromosomes condensed normally (Tram and Sullivan, 2002; Ferree and Sullivan, 2006; Landmann et al., 2009). It is likely that sperms derived from *Wolbachia*-infected males are modified during spermatogenesis, as CI-induced defects are limited to paternal chromosomes and *Wolbachia* are shed from mature sperm cells (Werren, 1996).

A number of host genes that are potentially influenced by *Wolbachia* infection (Landmann et al., 2009; Zheng et al., 2011b; Liu et al., 2014; Christensen et al., 2016; Wu et al., 2016), as well as *Wolbachia*'s prophage WO genes (cifA and cifB) that manipulate host reproduction (Beckmann et al., 2017; Lepage et al., 2017; Shropshire et al., 2018) have been identified. These genes provide a better understanding of the *Wolbachia*–host interaction. However, manipulation of host reproduction by *Wolbachia* is complex and involves many physiological processes (Serbus et al., 2008). Quantitative proteomic studies provide an opportunity to clarify these processes. *Wolbachia* infection is reported to significantly alter the expressions of proteins involved in metabolism, immunity, reproduction, transcriptional regulation, and protein modification/degradation (Baldridge et al., 2014, 2017; Yuan et al., 2015; Li et al., 2018). These differentially expressed proteins (DEPs) provide clues to the mechanisms underlying the *Wolbachia*-induced CI. Further functional analyses are needed to investigate the detail roles of these candidate proteins in reproductive manipulation.

* Corresponding author.
E-mail address: xyhong@njau.edu.cn (X.-Y. Hong).
[1] These authors contributed equally to this study.

https://doi.org/10.1016/j.ibmb.2019.103211
Received 10 May 2019; Received in revised form 4 July 2019; Accepted 24 July 2019
Available online 16 August 2019

The small brown planthopper (SBPH, *Laodelphax striatellus*) is a destructive pest that damages rice plants by feeding and transmitting viruses. Our previous work demonstrated that 100% of *L. striatellus* in China are infected with *Wolbachia* strain wStri (Zhang et al., 2013). The high *Wolbachia* infection rate was closely associated with their sophisticated reproduction strategies, with almost complete CI observed in laboratory-reared *L. striatellus* (Noda et al., 2001). In addition, *Wolbachia*-induced CI was durable, and strong CI can be caused even in aged male *L. striatellus* (Noda et al., 2001), which is significantly different from that of *Culex pipiens* (Subbarao et al., 1977) and *Drosophila simulans* (Hoffmann et al., 1986). *Wolbachia* improved the fecundity of infected *L. striatellus* (Guo et al., 2018b) and *Tribolium confusun* (Wade and Chang, 1995), but it decreased the fecundity of *Drosophila mauritiana* (Fast et al., 2011). The recent availability of the genome of *L. striatellus* (Zhu et al., 2017) provides an opportunity to study the mechanism of *Wolbachia*–induced CI in this notorious pest. Ju et al. (2017) found that, in *L. striatellus*, *Wolbachia*-induced CI was associated with reduced amino acid biosynthesis, especially the branched chain amino acids (BCAA), which delayed sperm maturation. However, the amino acid-deficiency model only partially explained the male infertility induced by *Wolbachia*-infection (Ju et al., 2017). Other factors that involved in *Wolbachia*–planthopper interactions still need further investigation.

In this study, we investigated the distribution of *Wolbachia* in the male gonads of *L. striatellus* and determined the adult stage with the highest *Wolbachia*-titer. Then, the global protein expression patterns of *Wolbachia*-infected and *Wolbachia*-uninfected *L. striatellus* were profiled by an isobaric tag for relative and absolute quantitation (iTRAQ) labeling method. The proteins that were differentially expressed upon *Wolbachia* infection were further analyzed and their corresponding transcript levels were assessed by qPCR. In addition, the functions of seven DEPs that were highly expressed in male gonads were investigated by RNA interference. We found that cytosol amino-peptidase-like protein (CAL) was influenced by *Wolbachia* infection, and might be one of the factors responsible for CI. Our results provide evidence that *Wolbachia*-induced CI might be caused by modification of reproductive proteins during spermatogenesis.

2. Material and methods

2.1. L. striatellus and Wolbachia strains

L. striatellus used in this study were originally collected from Nanjing, Jiangsu, China, and reared on fresh rice seedlings at 26 ± 0.5 °C with humidity at 50 ± 5% under a 16/8 h (light/dark) photoperiod. Previous study demonstrated that *L. striatellus* in China are 100% infected with *Wolbachia* (Zhang et al., 2013). Therefore, *Wolbachia*-uninfected strain used in this study was generated by tetracycline treatment (Noda et al., 2001), and confirmed to be *Wolbachia*-free by PCR amplification. Wild L. *striatellus* (with *Wolbachia*) and *Wolbachia*-free *L. striatellus* were maintained for over 30 generations on rice seedlings in a laboratory to eliminate any effects of residual tetracycline.

2.2. Immunofluorescence staining

Male gonads of *L. striatellus* were stained as previously described (Guo et al., 2018a). Briefly, male gonads were isolated from *L. striatellus* of different development stages in phosphate buffered saline (PBS, pH = 7.4), and fixed in 4% paraformaldehyde (v/v) for 30 min. Then, the tissues were blocked with 10% fetal bovine serum (Gibco, Grand Island, NY, USA) at room temperature for 1 h. The primary antibody against *Wolbachia* HSP-60 (Sigma, St. Louis, MO, USA) was added at a dilution of 1: 200 and incubated overnight at 4 °C. Following 3 times washes in PBS with 0.1% Triton-X-100, the samples were visualized with a tetramethylrhodamine isothiocyanate (TRITC)-coupled anti-mouse antibodies (1:200) (Sigma). For nucleus-specifc staining, the samples were stained with 100 nM of 4',6-diamidino-2-phenylindole (DAPI) (Yeasen, Shanghai, China) for 2 min. Fluorescence images were examined using a confocal laser scanning microscopy (Leica, Heidelberg, Germany).

2.3. Quantitative proteomic analysis

Approximately 250 pairs of male gonads were dissected from 4-day-old adults of *Wolbachia*-infected and uninfected *L. striatellus* under a stereomicroscope. The dissected testes were quickly washed in PBS and transferred into PBS containing Pierce Protease Inhibitor (Invitrogen, Grand Island, NY, USA). The samples were homogenated and underwent iTRAQ labeling analysis at the Beijing Genomics Institute (BGI), in Shenzhen, China. Briefly, the protein solution was diluted 4 times with 100 mM TEAB. After trypsin digestion, peptides were desalted with a Strata X C18 column and vacuum-dried. The peptides were labeled with respective isobaric tags and incubated for 2 h. Then, the iTRAQ labeled peptides were combined and desalted with a Strata X C18 column and vacuum-dried according to the manufacturer's protocol.

High-pH reversed-phase liquid chromatography separation and LC-MC/MC analysis was performed as previous described (Cheng et al., 2019).The generated raw MS/MS data was searched by Mascot search engine (Matrix Science, London, UK; version 2.3.02) against a protein database of *L. striatellus* (ftp://parrot.genomics.cn/gigadb/pub/10.5524/100001_101000/100361/), which contained 17,736 predicated proteins (Zhu et al., 2017). Several parameters in Mascot were set for peptide searching, including iTRAQ8plex for quantification, tolerance of two missed cleavages of trypsin, monoisotopic mass accuracy, carbamidomethyl (C), iTRAQ8plex (N-term), iTRAQ8plex (K) for cysteine as fixed modification, oxidation (M), and iTRAQ8plex (Y) for methionine as variable modification. In MS/MS mode, the fragment ion mass accuracy was set to < 0.1 Da. In MS/peptide mode, the peptide mass accuracy was set to < 0.05 Da.

iQuant method, including algorithms of Mascot and Percolator, was used for protein quantification (Wen et al., 2014). For peptide-to-spectrum match, peptides at the 95% confidence interval by a Mascot probability analysis greater than "identity" were counted as identified, all peptide identification was required to have a "false discovery rate" (PSM-level FDR) estimation of no higher than 1%. The confident peptides were matched with the selected protein database, and calculated by "the parsimony principle." According to this principle, only the simplest group of proteins which are sufficient to explain all the observed peptides are reported to be inferred (Zhang et al., 2007). The matched proteins were filtered at 1% FDR (false discovery rate) at the protein level and protein matches with at least one unique peptide were accepted as confident protein identification. The protein fold changes were reported as the median ratios of tag intensities of all significantly matched peptides. To investigate the differential expression of proteins between two treatments, the protein-relative abundance (ratio) was calculated, and only ratios with a P-value < 0.05 was accepted. The *Wolbachia*-infected *L. striatellus* replicate 1 (WI-1)/*Wolbachia*-uninfected *L. striatellus* replicate 1 (WU-1), WI-1/WU-2, WI-1/WU-3, WI-2/WU-1, WI-2/WU-2, WI-2/WU-3, WI-3/WU-1, WI-3/WU-2, WI-3/WU-3 were set as comparison groups. Ratios with fold changes > 1.20 or < 0.83 were considered as cases of differentially expressed proteins.

2.4. Enrichment analysis

The differentially expressed proteins were used for GO and KEGG enrichment analyses. Enriched P-values were calculated according to the hypergeometric test: $p = 1 - \sum_{i=0}^{m-1} \frac{\binom{M}{i}\binom{N-M}{n-i}}{\binom{N}{n}}$. In this equation, N represents the number of proteins with GO/KEGG annotation, n represents the number of differentially expressed proteins in N, M

represents the number of proteins in each GO/KEGG term, m represents the number of differentially expressed proteins in each GO/KEGG term. P-values after Bonferroni correction < 0.05 were used as a threshold to determine significant enrichment of the protein sets.

2.5. Quantitative PCR (qPCR)

Male gonads were dissected from 4-day-old adults of *Wolbachia*-infected and uninfected *L. striatellus* as described above. In addition, *L. striatellus* tissue of salivary glands (80), guts (50), fat body (50), carcass (30), male gonads (30) and ovaries (20) were also carefully dissected. The number of insects in each sample is illustrated in brackets. Total RNA was isolated using TRIzol Total RNA Isolation Kit (Takara, Dalian, China), and 500 ng RNA was reverse-transcribed in a 10-μl reaction system using HiScript Q RT Super Mix with a gDNA Remover Kit (Vazyme, Nanjing, China). qPCR was performed using primers designed by Primer Premier 6.0 (Table S1). The housekeeping genes for β-actin and GAPDH were used as internal control. Relative expression patterns were quantified by an ABI 7500 Real-Time PCR System (Applied Biosystems, Carlsbad, CA) using the SYBR Green Supermix Kit (Yeasen, Shanghai, China). The first-strand cDNA and a no-reverse-transcription control were used as templates under the following reaction program: denaturation for 5 min at 95 °C, followed by 40 cycles at 95 °C for 10 s and 60 °C for 30 s. Quantitative variation was evaluated with the $2^{-\Delta\Delta Ct}$ method (Livak and Schmittgen, 2001) using three independent biological replicates.

For determination of *Wolbachia* density, DNA was isolated from whole male *L. striatellus* and male gonads of different development stages using Wizard Genomic DNA Purification Kit (Promega, Madison, WI, USA). The DNA concentration was determined using a Nano-Drop 1000 spectrophotometer (Nano Drop Technologies, USA), and DNA was diluted to 5 ng/μl qPCR was performed as described above. *Wolbachia* genome copy number was determined by qPCR using primers specifically designed for the surface protein gene *wsp* of wStri (Table S1). *Glyceraldehyde-3-phosphate dehydrogenase* (*GAPDH*), *actin*, and *acetylcholinesterase* were used as reference genes. Three independent biological replicates were performed.

2.6. RNA interference (RNAi) experiment

The primers used for dsRNA synthesis are shown in Table S1. To minimize the non-target effect of RNAi, the target genes were searched against the transcriptomic and genomic database of *L. striatellus*, and the specific regions of the target genes were selected for dsRNA synthesis. After the target sequences were cloned into the pClone007 Vector (Tsingke, Beijing, China), the dsRNAs were synthesized from PCR-generated DNA templates using T7 High Yield RNA Transcription Kit (Vazyme). Fifth-instar *Wolbachia*-uninfected or *Wolbachia*-infected *L. striatellus* were treated with dsRNA by microinjection based on a previously reported method (Huang et al., 2018). Approximately 250 ng dsRNA was microinjected into the mesothorax of 5th instar nymphs. The majority (approximately 90%) of nymphs survived 24 h after injection. The dsRNA-treated insects were reared on rice seedlings, and the male *L. striatellus* were selected. One dsRNA-treated male *L. striatellus* was allowed to mate with one untreated female *L. striatellus* (not treated with dsRNA, virgin), and allowed to oviposit for 5 days. Five days later, the paired *L. striatellus* were transferred to new rice seedlings and oviposit for another 5 days. The number of hatched offspring and unhatched eggs in rice plants were counted.

2.7. Cell viability analysis

The dsRNA-treated male *L. striatellus* were anesthetized on ice. The vas deferens (VDs) of male gonads were dissected and washed in HEPES buffered saline solution (10 mM HEPES, 150 mM NaCl, 10% BSA, pH 7.4). Cell survival was assessed using a LIVE/DEAD Viability Kit (Molecular Probes, Eugene, OR) as previously described (Huang et al., 2018). Briefly, 5 μl diluted SYBR14 dye was added to 500 μl buffer and incubated for 5 min at 36 °C. Then, propidium iodide was added and incubated for another 5 min. The proportion of green cells (live) and red cells (dead) were counted using a confocal laser scanning microscopy. Each sample contained 8–10 individual insects, and each treatment was repeated for three independent experiments.

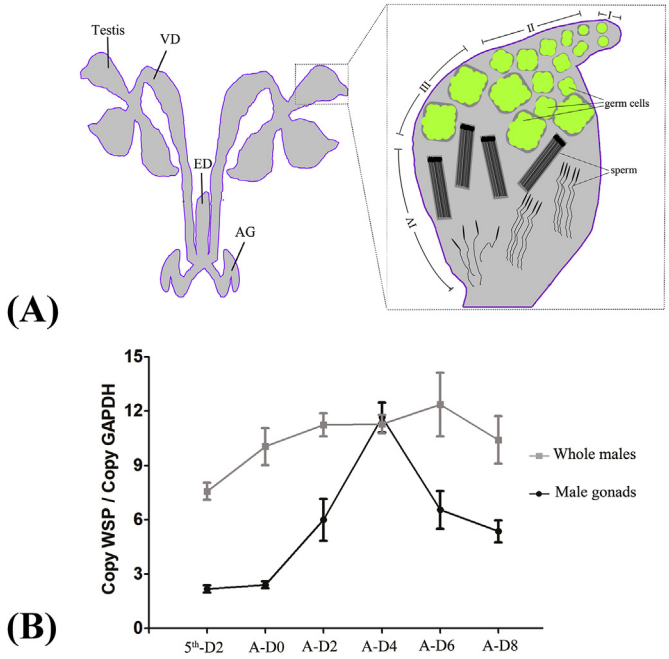

Fig. 1. Male gonads of *L. striatellus* and *Wolbachia* distribution. (A) A schematic diagram of male gonads of *L. striatellus*, which harbor two testes, two vas deferens (VDs), two accessory glands (AGs), and one ejaculatory duct (ED). Each testis contains three testicular tubules, where germ cells differentiate into sperms and transfer to VDs. According to the development of germ cells, testicular tubules can be divided into four zones (Lei and Rong, 2011): germarium zone (I), growth zone (II), maturation zone (III) and transformation zone (IV). (B) *Wolbachia* dynamics in whole male insects and male gonads from 5th instar male nymphs to 8-day-old male adults. *Glyceraldehyde-3-phosphate dehydrogenase* (*GAPDH*), *actin*, and *acetylcholinesterase* were used as reference genes. The representative result was showed as the ratio of copy numbers of *Wolbachia* wsp to host SBPH *GAPDH*. Bars: ± standard errors (SE).

3. Results

3.1. Density of Wolbachia in male gonads

The male gonads of *L. striatellus* consist of two testes, two vas deferens (VDs), two accessory glands (AGs), and one ejaculatory duct (ED) (Fig. 1A). They become visible at the late stage of 5th instar nymph. Each testis contains three testicular tubules, where spermatogenesis takes place and the germline stem cells (GSCs) differentiate into sperms. To understand the dynamic of *Wolbachia* titers during insect development, we monitored the *Wolbachia* density in whole male SBPHs and male gonads (Fig. 1B). A qPCR analysis showed that *Wolbachia* density in whole male SBPHs was relatively stable at the adult stages, and the 5th instar nymphs harbor less *Wolbachia* than do the adults. For male gonads, *Wolbachia* density was fairly low in 5th instar nymphs and newly emerged adults. The density increased rapidly after eclosion, with a relative transcript level reaching a peak on 4th day after eclosion (Fig. 1B).

Immunofluorescence staining clearly revealed the distribution of *Wolbachia* in the male gonads (Fig. 2). No signal was detected in the gonads of *Wolbachia*-uninfected control and *Wolbachia*-infected 5th

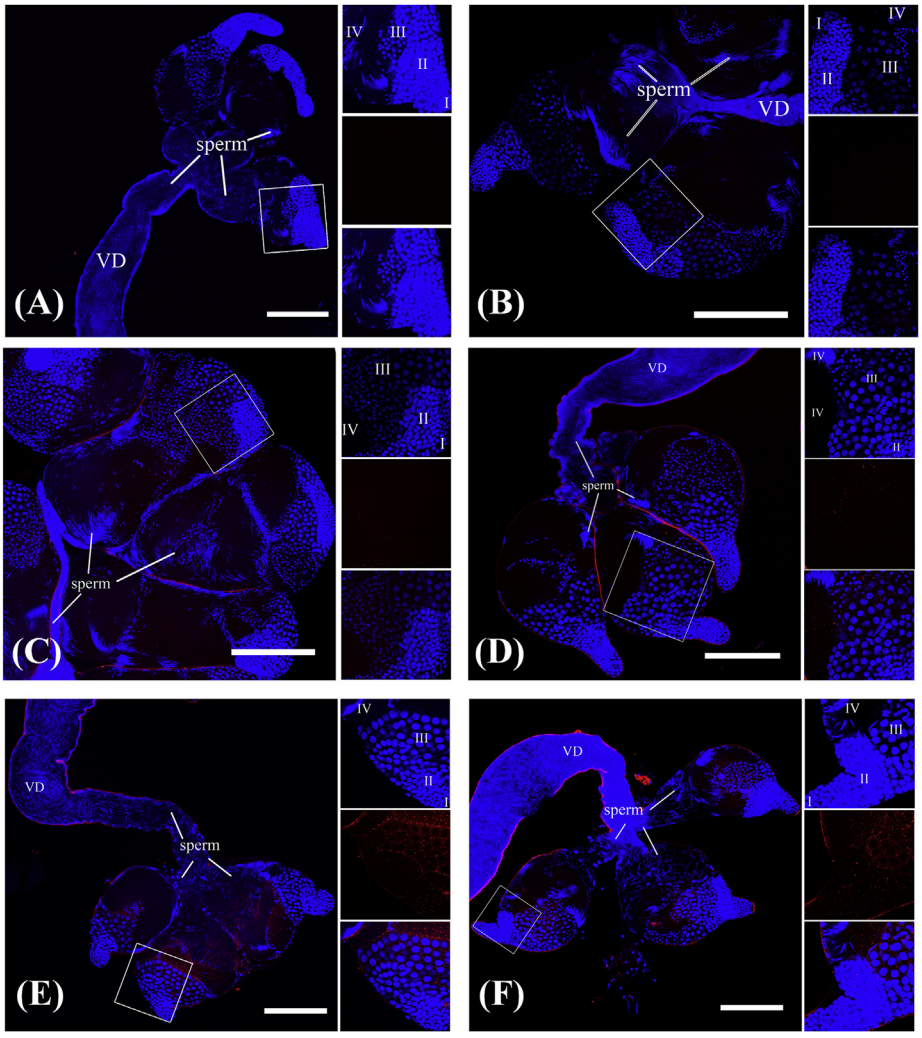

Fig. 2. Confirmation of *Wolbachia* infection by immunofluorescence staining analysis. The male gonads were dissected from *Wolbachia*-uninfected *L. striatellus* (A), *Wolbachia*-infected *L. striatellus* of 5th instar nymph (B), 0-day-old adult (C), 2-day-old adult (D), 4-day-old adult (E), and 6-day-old adult (F). Red fluorescence referred to *Wolbachia* that were stained with an antibody to Hsp-60. Blue fluorescence (DAPI) referred to the nuclei of gonad cells. I, germarium zone; II, growth zone; III, maturation zone; IV, transformation zone. Bars: 200 μm. (For interpretation of the references to colour in this figure legend, the reader is referred to the Web version of this article.)

instar nymphs (Fig. 2A and B). A *Wolbachia* signal was first detected in the testis of newly emerged adults, and only a small portion of germ cells were infected (Fig. 2C). The amount of *Wolbachia* increased dramatically on the 4th day after eclosion, with the majority of germ cells infected with *Wolbachia* (Fig. 2E). According to the development of germ cells, the testicular tubules are divided into four zones: germarium zone (I), growth zone (II), maturation zone (III) and transformation zone (IV) (Lei and Rong, 2011). *Wolbachia* were mainly distributed in the maturation and transformation zones, but some were observed in the germarium and growth zones (Fig. 2C–F). In addition, no *Wolbachia* signal was detected in the VDs, indicating that *Wolbachia* were stripped away from mature sperms. The *Wolbachia* distribution in male gonads on the 6th day was similar to that of the 4th day. However, their amount decreased, in agreement with the qPCR results.

3.2. iTRAQ-based protein identification and quantification

Based on the above observations of *Wolbachia* density, the male gonads isolated from 4 day-old *L. striatellus* were used to identify host proteins regulated by *Wolbachia*. A total of 317,500 spectra were generated by iTRAQ labeling, and 3,992 proteins were identified with a FDR < 1%. A principal component analysis (PCA) demonstrated that the three replicates of each treatment were well clustered (Fig. S1), indicating that *Wolbachia* has a non-negligible influence on the gonads. According to the criteria (fold change ratio > 1.2 and $p < 0.05$) for defining DEPs, a comparison of *Wolbachia*-infected *L. striatellus* and *Wolbachia*-uninfected *L. striatellus* identified 117 downregulated and 159 upregulated proteins (Table S2). The outer dense fiber protein (ODFP), which is the major component of the sperm tail cytoskeleton, was strongly upregulated in response to *Wolbachia*. In contrast, methyltransferase TARBP1, which participates in RNA modification, was strongly downregulated. In addition, three BCAA metabolism-related proteins (propionyl-CoA carboxylase, methylglutaconyl-CoA hydratase, and aldehyde dehydrogenase) were differentially expressed, in agreement with previous reports (Ju et al., 2017).

By performing GO enrichment analysis, DEPs were significantly enriched in 23 GO clusters with a p-value < 0.05 (Fig. 3). In the category cellular components, proteins associated with transcription factor complex, extracellular region, extracellular matrix were significantly enriched. In the category molecular function, most DEPs were associated with nucleotidyltransferase activity, ligase activity, and transcription regulator activity. In biological process, the majority of enriched GO terms were associated with modification, which included peptidyl-amino acid modification, cellular protein modification, protein modification, macromolecule modification, tRNA modification, and histone modification. According to the KEGG classification, 9 gene sets were significantly enriched with a p-value < 0.05 (Table S3). Gene sets associated with metabolic pathways were significantly enriched, including vitamin metabolism, glycerophospholipid metabolism, and pyrimidine metabolism.

3.3. Correlation between mRNA expression and protein abundance

To evaluate whether iTRAQ results are consistent with transcript

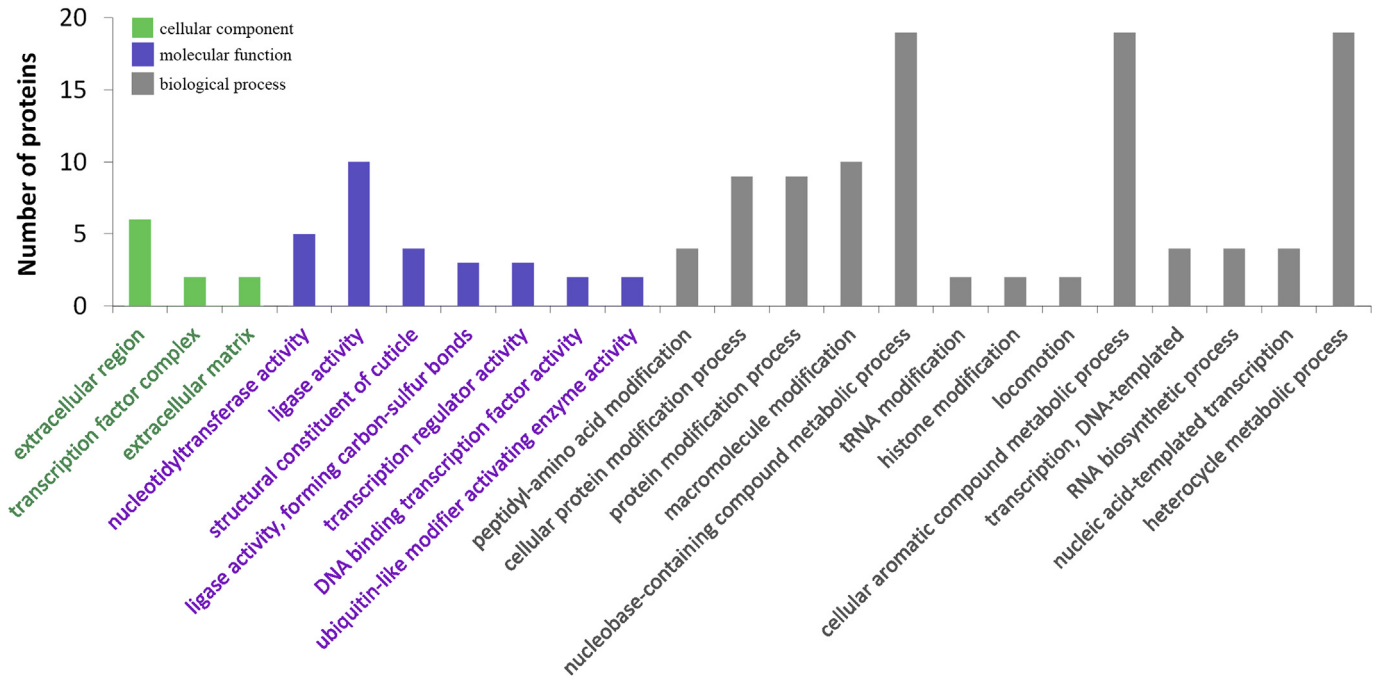

Fig. 3. Gene ontology (GO) classification of DEPs. Proteins were classified into three main categories: cellular component (CC), molecular function (MF), and biological process (BP). The GO terms with a p-value < 0.05 were shown.

levels, 12 DEPs were selected to perform qPCR analysis. Nine genes shared similar tendencies in mRNA expression and protein abundance (Fig. 4). The ODFP, which was upregulated 6.73-fold at the protein level, was upregulated 5.03-fold at the mRNA level. However, the fold change of several proteins was higher at the mRNA level than at the protein level. These included serine/threonine-protein phosphatase (STPP), histidine-tRNA ligase (HTL), mediator of RNA polymerase II transcription (MRPT), deoxynucleoside triphosphate triphosphohydrolase (DTT), venom allergen 5-like (VA5L), and cytochrome *b-c*1 complex subunit (CytB). Although some quantitative differences were observed in the proteomic and qPCR data, their similarities indicated that the proteomic data are reproducible and reliable .

3.4. Tissue-specific expression pattern of DEPs

We investigated the gene expression patterns of the 45 most differentially expressed proteins. Among them, VA5L and chemosensory protein CSP3 (CSP3) were exclusively expressed in male gonads. Other 5 genes, including ODFP, CytB, CAL, endoplasmic reticulum resident protein (ERRP), and an uncharacterized protein (UnP), expressed highest in male gonads. We mainly focused on these seven genes in the following experiment (Fig. 5).

3.5. Function of DEPs in reproduction

RNAi was used to investigate the biological functions of seven genes on male reproductivity. dsRNAs of green fluorescent protein (GFP) and target genes were synthesized and injected into the mesothorax of 5th instar males. Knockdown effects were determined 4 days after injection, and the results showed that the dsRNAs could efficiently suppress the expression of target genes (Fig. S2).

For *Wolbachia*-uninfected *L. striatellus*, the male nymphs treated with ds*VA5L* (~81 eggs per pair) and ds*ODFP* (~80 eggs per pair) produce less eggs than that of ds*GFP* control (~119 eggs per pair) (Fig. 6A). No significant influence was observed on other dsRNA treatments, with egg productions ranging from 114 to 137 per pair. Compared with ds*GFP* control (82.8%), injection of ds*CAL*(62.5%) significantly decreased the egg hatch rate, with the majority of unhatched eggs showing no eyespot (Fig. 6B and C). The eyespot, an indicator of viability during embryonic development, was visible at the 5th day of the embryonic stage (Fig. S3A). (The total development time of *L. striatellus* egg is approximately 7 days.) In contrast, the eggs derived from CI crosses showed no eyespot (Fig. S3B). In the ds*CAL* treatment, 25.9% of the eggs died at the early stage of embryonic development (without eyespot), which was significantly higher than that of ds*GFP* control (2.1%). In addition, the egg phenotypes of ds*CAL* treatment in different days were either similar with ds*GFP* treatment (~75% of total eggs examined) (Fig. S3C) or CI cross (~25% of total eggs examined) (Fig. S3D). In contrast, no significant difference was observed on egg hatch rate in other dsRNA treatments.

For *Wolbachia*-infected *L. striatellus*, the male nymphs treated with ds*VA5L* (~91 eggs per pair) and ds*ODFP* (~111 eggs per pair) significantly decreased the egg production (Fig. 7A), similar with that of *Wolbachia*-uninfected strain. However, we did not find a significant difference in hatch rate between ds*GFP* control and other dsRNA treatments (Fig. 7B and C). Although the portion of dead embryos without eyespots in the ds*CAL* treatment (3.7%) was slightly higher than that in the ds*GFP* control (1.7%) (Fig. 7C), the difference was not significant.

As ds*CAL* treatment well mimicked the *Wolbachia*-induced CI, dsRNA-treated *Wolbachia*-uninfected males were also crossed with *Wolbachia*-infected females. Egg production, egg hatch rate, and the portion of dead embryos without eyespots were not significantly different between ds*CAL*-treated and ds*GFP*-treated *Wolbachia*-uninfected males (Fig. S4).

We did not find any phenotype changes in whole insect or male gonads among the ds*GFP*, ds*CAL*, ds*VA5L*, and ds*ODFP* treatments (data not shown). The LIVE/DEAD staining analysis showed that 16.1% of sperms underwent severe cell death after ds*ODFP* treatment, which was significantly higher than that of ds*GFP* control (4.0%). In contrast, treatment with ds*CAL* and ds*VA5L* did not influence sperm viability (Fig. 8).

4. Discussion

Previous reports demonstrated that CI was caused by delayed

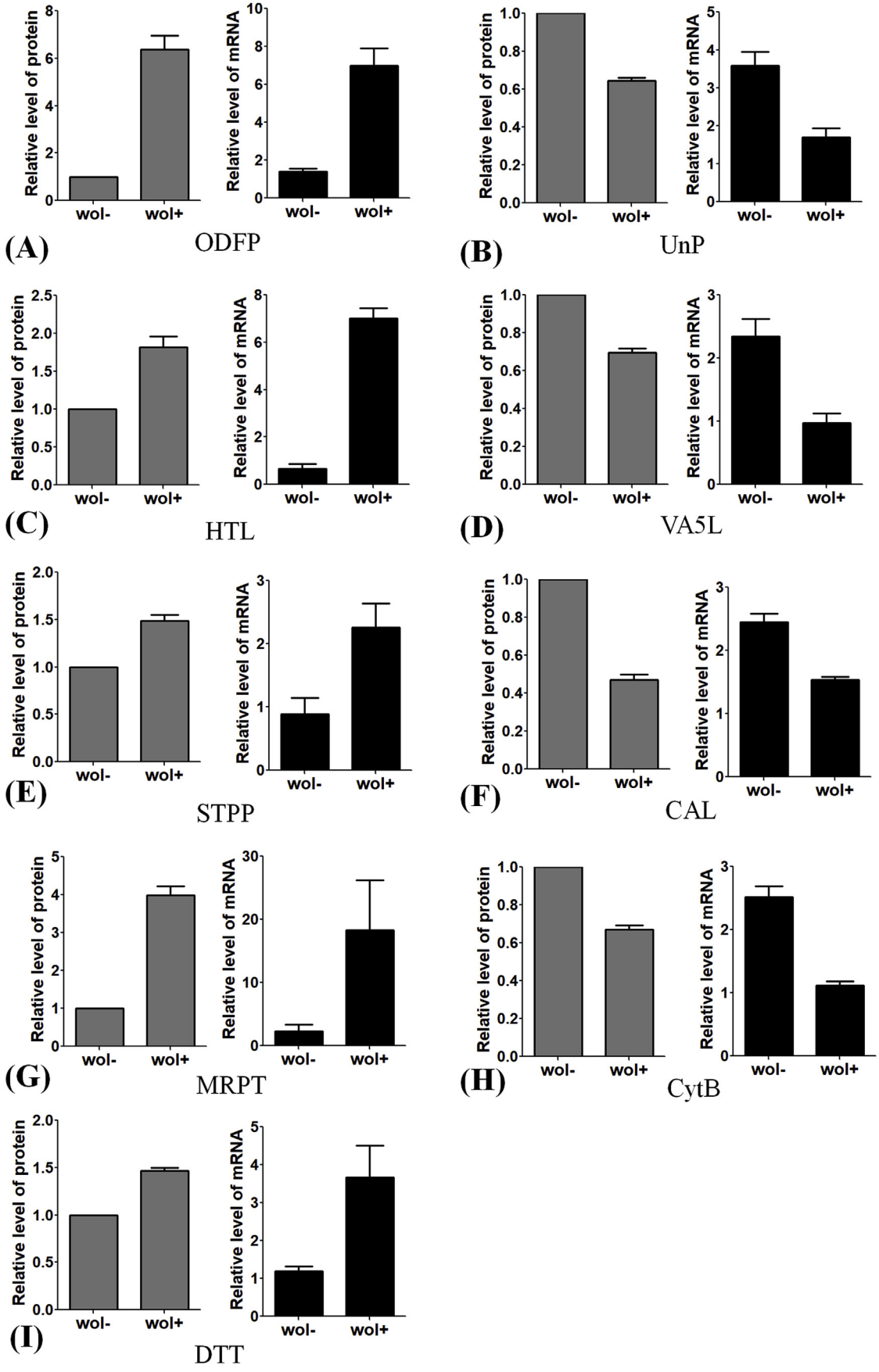

(caption on next page)

Fig. 4. Correlation between mRNA expression and protein abundance. Relative expression level of mRNA was determined by qPCR (black), and calculated using a relative quantitative method ($2^{-\Delta\Delta Ct}$) (Livak and Schmittgen, 2001). The relative abundance (ratio) of each protein was determined by iTRAQ labeling analysis, and quantified using iQuant method (Wen et al., 2014). (A) outer dense fiber protein (ODFP); (B) uncharacterized protein (UnP); (C) histidine-tRNA ligase (HTL); (D) venom allergen 5-like (VA5L); (E) serine/threonine-protein phosphatase (STPP) (F) cytosol amino-peptidase-like (CAL); (G) mediator of RNA polymerase II transcription (MRPT); (H) cytochrome *b*-*c*1 complex (CytB); (I) deoxynucleoside triphosphate triphosphohydrolase (DTT). Bars: ± standard errors (SE).

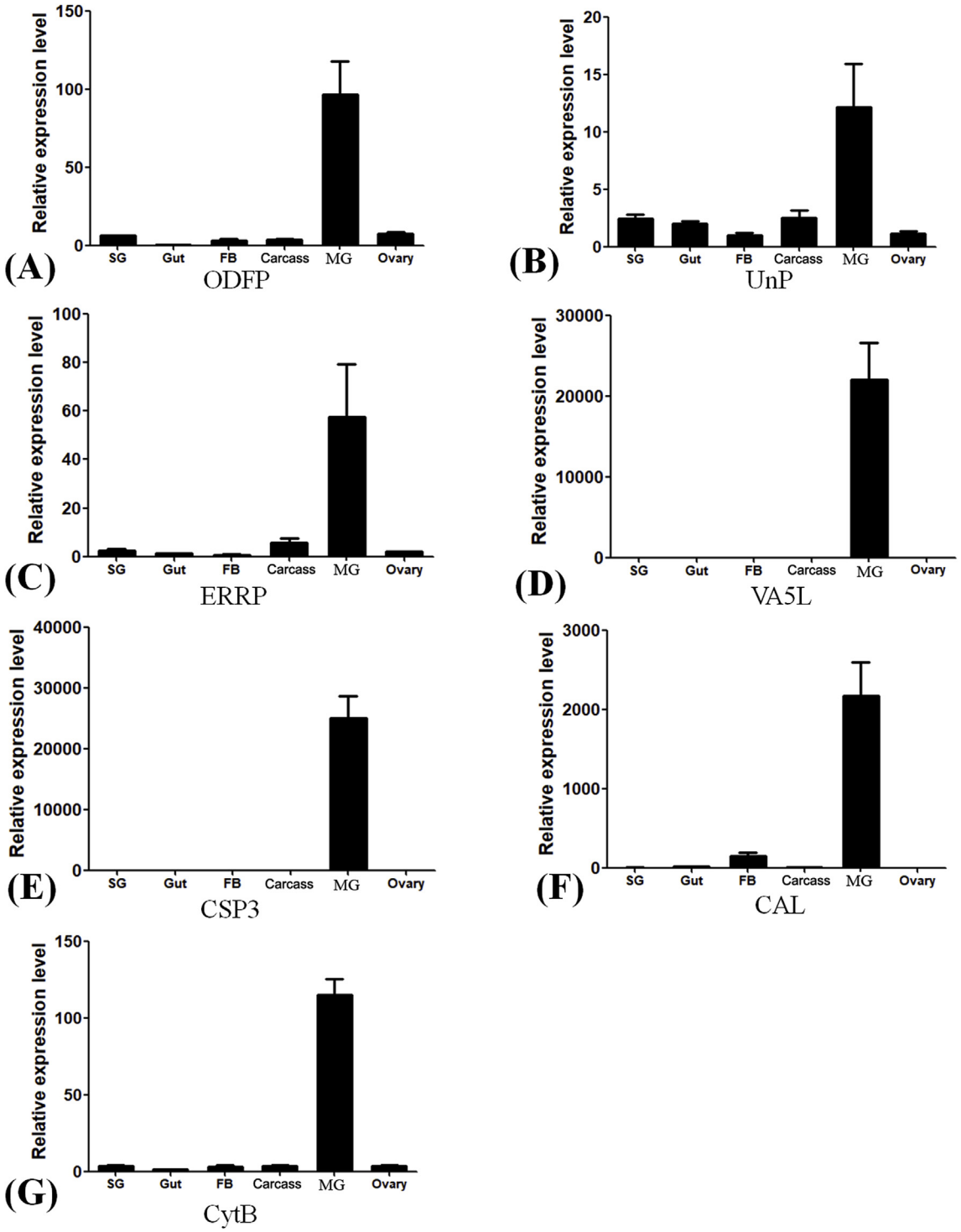

Fig. 5. Tissue-specific expression pattern of DEPs. Total RNA was extracted from salivary glands (SG), guts, fat bodies (FB), carcass, male gonads (MG), and ovaries. The expression patterns of genes were determined by qPCR, and calculated using a relative quantitative method ($2^{-\Delta\Delta Ct}$) (Livak and Schmittgen, 2001). Seven gonad high-expressed genes were exhibited. (A) outer dense fiber protein (ODFP); (B) uncharacterized protein (UnP); (C) endoplasmic reticulum resident protein (ERRP); (D) venom allergen 5-like (VA5L); (E) chemosensory protein CSP3 (CSP3); (F) cytosol amino-peptidase-like (CAL); (G) cytochrome *b*-*c*1 complex (CytB). Bars: ± standard errors (SE).

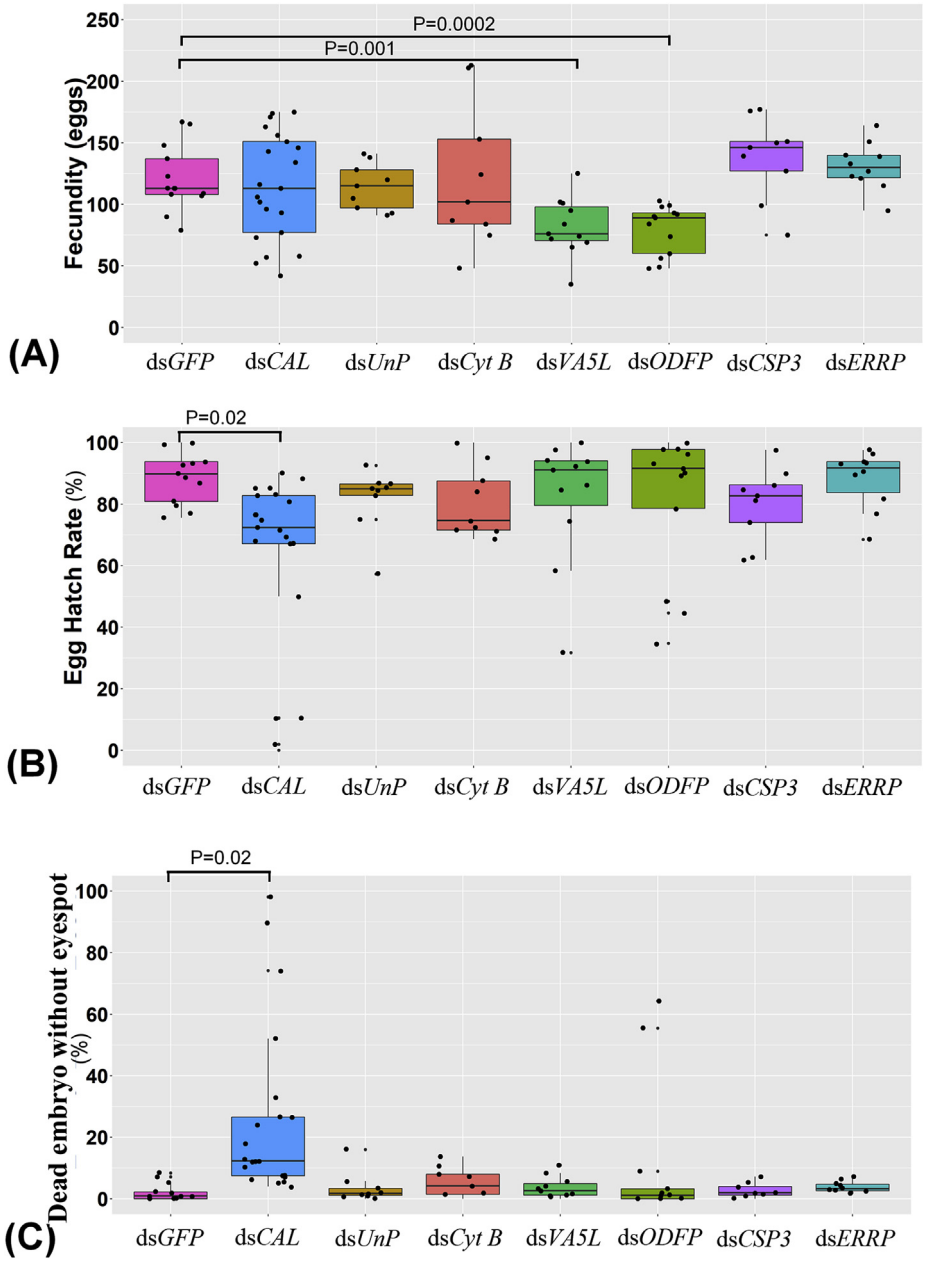

Fig. 6. Effect of dsRNA-treated *Wolbachia*-uninfected males crossed with *Wolbachia*-uninfected females. (A) The number of laid eggs per insect; (B) Percentage of hatched embryo; (C) Percentage of dead embryo without eyespot. The interquartile range is bordered by upper and lower edges, corresponding the 75th and 25th percentiles, respectively. Each point represents a biological replicate. $P < 0.05$ was considered statistically significant according to Student's t-test.

condensation of chromosomes derived from paternal, and modification of sperm during spermatogenesis might be critical for induction of CI (Tram and Sullivan, 2002; Ferree and Sullivan, 2006; Landmann et al., 2009). In the present study, we found that *Wolbachia* were distributed in the male gonads of *L. striatellus* after eclosion and peaked on the 4th day after eclosion. Therefore, we chose male gonads isolated from 4 day-old adults for proteomic analysis. Functional analysis of seven DEPs highly expressed in the gonads showed that knocking down the expression of *CAL* had negative effect on egg hatch rate in *Wolbachia*-uninfected males, and appropriately 25% of eggs from ds*CAL* treatments showed phenotypes similar with that of CI crosses. Because *Wolbachia* suppressed *CAL* expression, we speculated that *CAL* might be correlated with the induction of CI in *L. striatellus*.

The male gonads become visible in 5th instar nymphs and the *Wolbachia* concentration is high in whole *L. striatellus* at this stage. However, we did not observe a wide distribution of *Wolbachia* in the male gonads (Figs. 1 and 2), possibly because of the barriers (circumferential muscle and terminal epithelium) surrounding the testis (Clark et al., 2002). Although *Wolbachia* resided along within spermatocytes on the 4th day, the majority of sperms produced in the first 2 days did not come in direct contact with these endosymbionts. In *N. vitripennis*, *Wolbachia* modified nearly all sperms, but were found in only ~28% of the spermatocytes (Clark et al., 2008); in *Chelymorpha alternans*, *Wolbachia* modified ~ 90% of sperms, but were never observed within the developing sperms (Clark et al., 2008). Our results provide additional evidence that sperm modification may not always require the presence of *Wolbachia* within developing sperms. This might partially explain the durability of CI in *L. striatellus*: even though the density of *Wolbachia* in the gonads decreased in aged males, it was still high enough to cause 100% CI (Noda et al., 2001).

Comparative proteomic analyses revealed that DEGs involved in vitamin metabolism, lipid metabolism, and nucleotide metabolism were

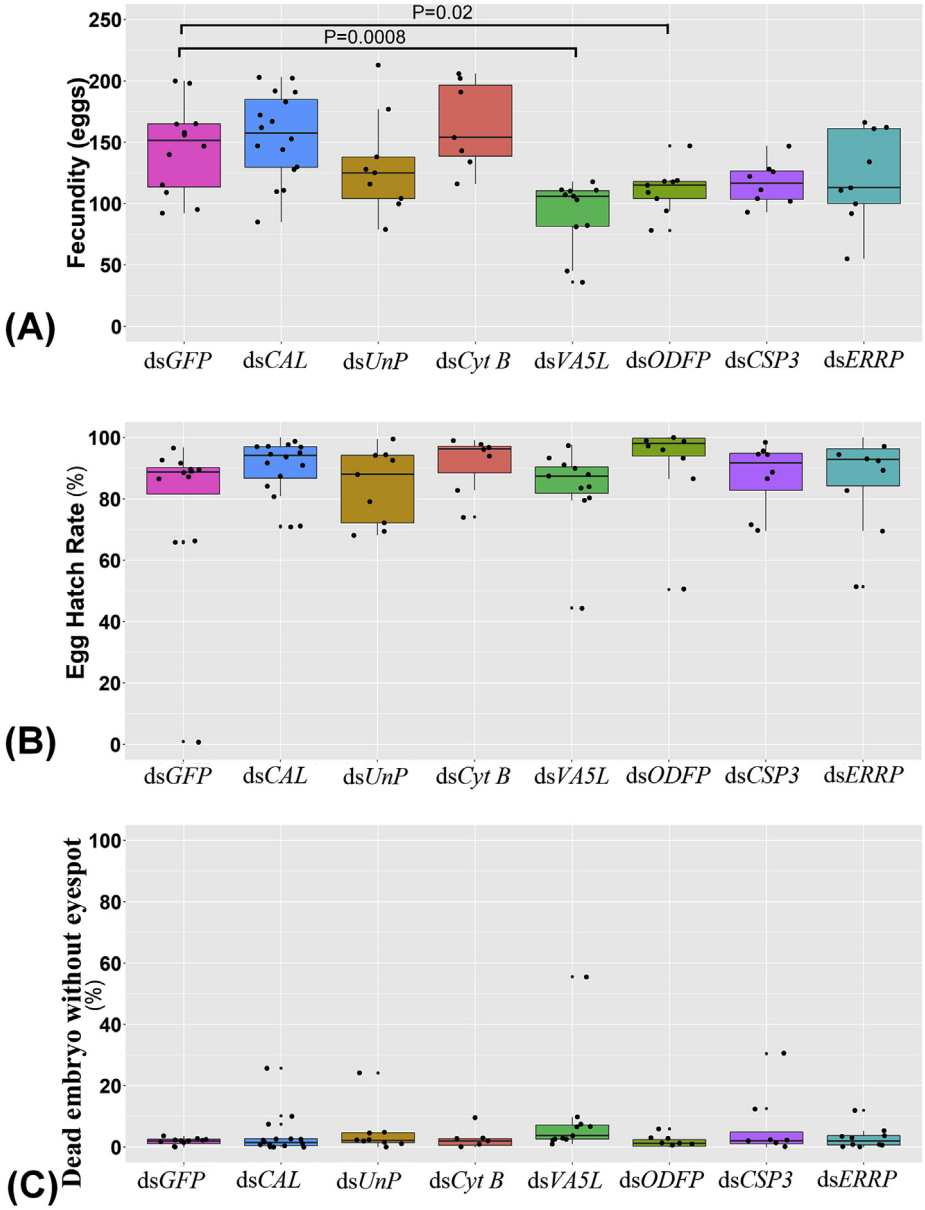

Fig. 7. Effect of dsRNA-treated *Wolbachia*-infected males crossed with *Wolbachia*-infected females. (A) The number of laid eggs per insect; (B) Percentage of hatched embryo; (C) Percentage of dead embryo without eyespot. The interquartile range is bordered by upper and lower edges, corresponding the 75th and 25th percentiles, respectively. Each point represents a biological replicate. P < 0.05 was considered statistically significant according to Student's t-test.

significantly altered. *Wolbachia* are intracellular bacteria that have evolved intimate mutualistic associations with their hosts (Fenn and Blaxter, 2006). They obtain some metabolites from host cells, which may influence the expression of corresponding genes (Serbus et al., 2008). In *Aedes albopictus*, changes in proteins associated with amino acid metabolism, vitamin metabolism, and nucleotide metabolism were reported in response to *Wolbachia* infection (Baldridge et al., 2017); while, in *Nasonia vitripennis*, *Wolbachia* infection lead to alteration in alpha-linolenic acid metabolism, ether lipid metabolism, and carbon metabolism (Li et al., 2018). In this study, the majority of DEPs associated with lipid transport and metabolism were significantly upregulated upon *Wolbachia* infection. These included three lipases that catalyze the hydrolysis of fatty acids. *Wolbachia* have a highly reduced genome with limited lipid metabolic capabilities (Wu et al., 2004). Substantial shifts in the cellular lipid profiles have been observed in the presence of *Wolbachia* in *Aedes albopictus* cells (Molloy et al., 2016). The altered lipid metabolism in *L. striatellus* might be the result of lipid consumption by *Wolbachia*, with hosts having to increase the biosynthesis of the consumed metabolite (Zheng et al., 2011b). In addition, some hosts also depend on *Wolbachia* for nutrition, e.g., *Wolbachia* in *Cimex lectularius* provided vitamin B that was essential for host development (Moriyama et al., 2015); *Wolbachia* in *Aedes fluviatilis* facilitated embryonic development by modulating glycogen metabolism (da Rocha Fernandes et al., 2014). *L. striatellus* receives a reproductive benefit from *Wolbachia* (Guo et al., 2018b). Further studies are needed to see if this benefit is correlated with metabolic modulation.

A notable finding of the GO analysis was the enrichment of gene sets related to modification (Fig. 3). CI has been well interpreted by the "modification-rescue" model, in which bacteria present in the testes modify the developing sperm, while the same bacterial strain must be present in the egg to rescue this modification (Werren, 1996; Beckmann et al., 2019). Modification of sperms leads to a defect in CI cross, and chromosomes derived from paternal delayed in condensation (Tram and Sullivan, 2002). Ultra-structural observations confirmed the morphological changes in developing sperm, including abnormal mitochondria and axonemes (Riparbelli et al., 2007). It has been reported

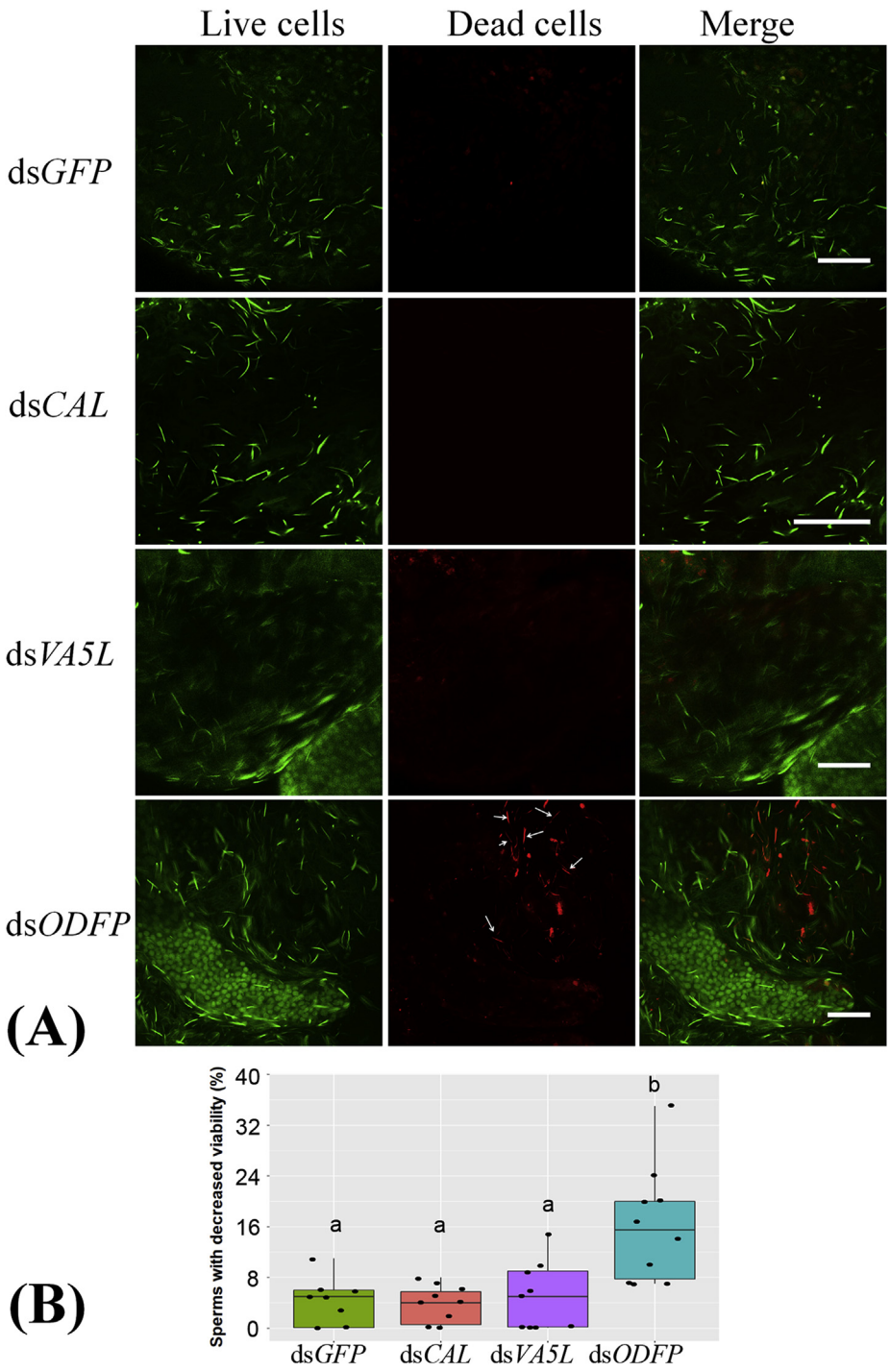

Fig. 8. Effect of dsRNA treatment on sperm viability. *Wolbachia*-uninfected males were treated with dsRNA, and sperm viability was determined 5 days later using LIVE/DEAD staining. (A) Representative fluorescent signal of male gonad. Live sperms fluoresce green, whereas dead sperms fluoresce red. (B) Quantification of sperm viability. For each treatment, the sperms that experienced decreased viability were counted and expressed as a percentage of the examined sperms. The interquartile range is bordered by upper and lower edges, corresponding the 75th and 25th percentiles, respectively. Each point represents a biological replicate. Different letters indicate significant differences among each treatment group at $P < 0.05$ according to one-way ANOVA test. White arrows indicated dead sperms fluoresce red. (For interpretation of the references to colour in this figure legend, the reader is referred to the Web version of this article.)

that proteins associated with protein/RNA modification were differentially expressed upon *Wolbachia* infection (Baldridge et al., 2014, 2017). In this study, we found a large amount of proteins involved in histone modification, peptidyl-amino acid modification, macromolecule modification, and tRNA modification altered. Histones are the chief protein components of chromatin (Fischle et al., 2003). Histone modifications play critical roles in most biological processes that involve the manipulation and expression of DNA (Bannister and Kouzarides, 2011). In *D. simulans*, CI phenotype was associated with impaired histone deposition (Frédéric et al., 2009). In *D. melanogaster*, a decreased expression of histone chaperone in male flies might be responsible for *Wolbachia*-induced CI (Zheng et al., 2011a). An altered histone modification in male *L. striatellus* might regulate gene expressions during spermatogenesis, which could delay chromosome condensation.

Seven proteins that are highly expressed in the gonads were differentially expressed. Outer dense fiber proteins (ODFPs) are major components of sperm tail, which maintain elastic recoil of sperms and protect sperms against shearing forces during epididymal transport (Baltz et al., 1990). Venom allergen 5-like (VA5L) contains a sperm coating protein (SCP) domain, and was reported to be the main component of seminal fluid in planthoppers (Chalmers et al., 2008; Yu et al., 2016). In this study, the mRNA and protein levels of ODFP were significantly higher in *Wolbachia*-infected gonads than in uninfected gonads, while the opposite was found for VA5L (Fig. 4). These two proteins influenced egg production, but not the hatch rate (Figs. 6 and 7),

which was significantly different from that of the CI phenotype. LIVE/DEAD staining showed that ODFP was critical for sperm viability (Fig. 8), and the insufficient viable sperms in ds*OPFP* treatment might be the cause of decreased egg production. We presumed that regulation of ODFP and VA5L was responsible for the *Wolbachia*-improved fecundity of *L. striatellus*, but that it was not the determinant of CI.

For ds*CAL* treatment, significant decreased in egg hatch rate was observed in *Wolbachia*-uninfected *L. striatellus* (Fig. 6). The majority of unhatched eggs died at the early stage of embryonic development, as did the eggs of the CI phenotype. Because mRNA/protein level of CAL was significantly downregulated in *Wolbachia*-infected male gonads (Fig. 4), knocking down the expression of *CAL* in *Wolbachia*-uninfected males well mimicked the effect of *Wolbachia* on this gene. In contrast, the egg hatch rate was not significantly different between ds*CAL*-treated and ds*GFP*-treated *Wolbachia*-infected males crossed with *Wolbachia*-infected females, or between ds*CAL*-treated and ds*GFP*-treated *Wolbachia*-uninfected males crossed with *Wolbachia*-infected females (Fig. 7, Fig. S4). These results indicated that regulation of CAL by *Wolbachia* might be critical for CI phenotype. CAL proteins are a kind of amino-peptidases that are extensively distributed in animal sperms (Simmons et al., 2013; Steve et al., 2006). In *Mytilus edulis* (Togo and Morisawa, 2004) and *Strongylocentrotus intermedius* (Yasuhara et al., 1991), amino-peptidases were found to be involved in the acrosome reaction that occurs as the acrosome approaches the egg. Our study found a decline in CAL level upon *Wolbachia* infection, and the sperms derived from *Wolbachia*-infected males might be deficient in CAL. This "CAL modification" might delay the entrance and condensation of paternal chromosomes, resulting in asynchronization of chromosomal condensation at the first mitosis. However, knocking down *CAL* did not achieve 100% embryo mortality as the CI crosses did. Further studies are needed to identify other factors that participate in CI.

In summary, we identified 276 DEPs associated with *Wolbachia* infection in male gonads of *L. striatellus*. Genes that related to metabolism, modification, and reproduction were significantly modulated. The altered expression of ODFP and VA5L might be responsible for the *Wolbachia*-improved fecundity in infected males, while the downregulation of CAL in male gonads might be one of the factors responsible for the CI phenotype.

Conflicts of interest

All authors have no conflicts of interest to declare.

Author contributions

H-J H and X–Y H planned and designed the research. J-R C, H-J H, J C and X-L B performed experiments and analyzed data. H-J H wrote the manuscript.

Acknowledgement

This work was supported by the National Natural Science Foundation of China (31801734, 31871976), the Fundamental Research Funds for the Central Universities (KJQN201914), and the Natural Science Foundation of Jiangsu Province (BK20180520).

Appendix A. Supplementary data

Supplementary data to this article can be found online at https://doi.org/10.1016/j.ibmb.2019.103211.

References

Baldridge, G., Baldridge, A., Witthuhn, B., Higgins, L.A., Markowski, T., Fallon, A., 2014. Proteomic Profiling of a Robust *Wolbachia* Infection in an *Aedes albopictus* Mosquito Cell Line, vol. 93. pp. 537–556.

Baldridge, G., Higgins, L.A., Witthuhn, B., Markowski, T., Baldridge, A., Armien, A., Fallon, A., 2017. Proteomic analysis of a mosquito host cell response to persistent *Wolbachia* infection. Res. Microbiol. 168, 609–625.

Baltz, J.M., Williams, P.O., Cone, R.A., 1990. Dense fibers protect mammalian sperm against damage. Biol. Reprod. 43, 485.

Bannister, A.J., Kouzarides, T., 2011. Regulation of chromatin by histone modifications. Cell Res. 21, 381.

Beckmann, J.F., Ronau, J.A., Hochstrasser, M., 2017. A *Wolbachia* deubiquitylating enzyme induces cytoplasmic incompatibility. Nat. Microbiol. 2, 17007.

Beckmann, J.F., Bonneau, M., Chen, H., Hochstrasser, M., Poinsot, D., Merçot, H., Weill, M., Sicard, M., Charlat, S., 2019. The toxin–antidote model of cytoplasmic incompatibility: genetics and evolutionary implications. Trends Genet. 35, 175–185.

Chalmers, I.W., Mcardle, A.J., Coulson, R.M., Wagner, M.A., Schmid, R., Hirai, H., Hoffmann, K.F., 2008. Developmentally regulated expression, alternative splicing and distinct sub-groupings in members of the *Schistosoma mansoni* venom allergen-like (SmVAL) gene family. BMC Genomics 9 89-89.

Cheng, Y., Mao, Y., Zheng, X., Liu, C., Liu, J., 2019. iTRAQ protein profiling reveals candidate proteins regulating ovary and ovule differentiation in pistillate inflorescences after pollination in hazel. Tree Genet. Genomes 15, 21.

Christensen, S., Dulzaides, R.P., Hedrick, V.E., Momtaz, A.J.M.Z., Nakayasu, E.S., Paul, L.N., Serbus, L.R., 2016. Wolbachia endosymbionts modify *Drosophila* ovary protein levels in a context-dependent manner. Appl. Environ. Microbiol. 82, 5354–5363.

Clark, M.E., Veneti, Z., Bourtzis, K., Karr, T.L., 2002. The distribution and proliferation of the intracellular bacteria *Wolbachia* during spermatogenesis in *Drosophila*. Mech. Dev. 111, 3–15.

Clark, M.E., Bailey-Jourdain, C., Ferree, P.M., England, S.J., Sullivan, W., Windsor, D.M., Werren, J.H., 2008. *Wolbachia* modification of sperm does not always require residence within developing sperm. Heredity 101, 420–428.

da Rocha Fernandes, M., Martins, R., Costa, E.P., Pacidônio, E.C., de Abreu, L.A., da Silva Vaz Jr., I., Moreira, L.A., da Fonseca, R.N., Logullo, C., 2014. The modulation of the symbiont/host interaction between *Wolbachia pipientis* and *Aedes fluviatilis* embryos by glycogen metabolism. PLoS One 9, e98966.

Fast, E.M., Toomey, M.E., Kanchana, P., Danielle, D., Kolaczyk, E.D., Frydman, H.M., 2011. *Wolbachia* enhance *Drosophila* stem cell proliferation and target the germline stem cell niche. Science 334, 990–992.

Fenn, K., Blaxter, M., 2006. *Wolbachia* genomes: revealing the biology of parasitism and mutualism. Trends Parasitol. 22, 60–65.

Ferree, P.M., Sullivan, W., 2006. A genetic test of the role of the maternal pronucleus in *Wolbachia*-induced cytoplasmic incompatibility in *Drosophila melanogaster*. Genetics 173, 839–847.

Fischle, W., Wang, Y., Allis, C.D., 2003. Histone and chromatin cross-talk. Curr. Opin. Cell Biol. 15, 172–183.

Frédéric, L., Orsi, G.A., Benjamin, L., William, S., 2009. *Wolbachia*-mediated cytoplasmic incompatibility is associated with impaired histone deposition in the male pronucleus. PLoS Pathog. 5, e1000343.

Guo, Y., Hoffmann, A.A., Xu, X.Q., Mo, P.W., Huang, H.J., Gong, J.T., Ju, J.F., Hong, X.Y., 2018a. Vertical transmission of *Wolbachia* is associated with host vitellogenin in *Laodelphax striatellus*. Front. Microbiol. 9.

Guo, Y., Hoffmann, A.A., Xu, X.Q., Zhang, X., Huang, H.J., Ju, J.F., Gong, J.T., Hong, X.-Y., 2018b. *Wolbachia*-induced apoptosis associated with increased fecundity in *Laodelphax striatellus* (Hemiptera: Delphacidae). Insect Mol. Biol. 27, 796–807.

Hilgenboecker, K., Hammerstein, P., Schlattmann, P., Telschow, A., Werren, J.H., 2008. How many species are infected with *Wolbachia* ? - a statistical analysis of current data. FEMS Microbiol. Lett. 281, 215–220.

Hoffmann, A.A., Turelli, M., Simmons, G.M., 1986. Unidirectional incompatibility between populations of *Drosophila* simulans. Evolution 40, 692–701.

Hoffmann, A.A., Turelli, M., Harshman, L.G., 1990. Factors affecting the distribution of cytoplasmic incompatibility in *Drosophila simulans*. Genetics 126, 933–948.

Huang, H.J., Cui, J.R., Guo, Y., Sun, J.T., Hong, X.Y., 2018. Roles of LsCYP4DE1 in wheat adaptation and ethiprole tolerance in *Laodelphax striatellus*. Insect Biochem. Mol. Biol. 101, 14–23.

Ju, J.F., Hoffmann, A.A., Zhang, Y.K., Duan, X.Z., Guo, Y., Gong, J.T., Zhu, W.C., Hong, X.Y., 2017. *Wolbachia*-induced loss of male fertility is likely related to branch chain amino acid biosynthesis and iLvE in *Laodelphax striatellus*. Insect Biochem. Mol. Biol. 85, 11–20.

Landmann, F., Guillermo, Orsi, Loppin, B., Sullivan, W., 2009. *Wolbachia*-mediated cytoplasmic incompatibility is associated with impaired histone deposition in the male pronucleus. PLoS Pathog. 5, e1000343.

Lei, C.L., Rong, X.L., 2011. In: General Entomology, Second. China Agriculture Press.

Lepage, D.P., Metcalf, J.A., Bordenstein, S.R., On, J., Perlmutter, J.I., Shropshire, J.D., Layton, E.M., Funkhouser-Jones, L.J., Beckmann, J.F., 2017. Prophage WO genes recapitulate and enhance *Wolbachia*-induced cytoplasmic incompatibility. Nature 543, 243–247.

Li, J., Wang, N., Liu, Y., Qiu, S., 2018. Proteomics of *Nasonia vitripennis* and the effects of native *Wolbachia* infection on. *N. vitripennis*. PeerJ 6, e4905.

Liu, C., Wang, J.L., Zheng, Y., Xiong, E.J., Li, J.J., Yuan, L.L., Yu, X.Q., Wang, Y.F., 2014. *Wolbachia*-induced paternal defect in *Drosophila* is likely by interaction with the juvenile hormone pathway. Insect Biochem. Mol. Biol. 49, 49–58.

Livak, K.J., Schmittgen, T.D., 2001. Analysis of relative gene expression data using real-time quantitative PCR and the $2^{-\Delta\Delta CT}$ method. Methods 25, 402–408.

Molloy, J.C., Sommer, U., Viant, M.R., Sinkins, S.P., 2016. *Wolbachia* modulates lipid metabolism in *Aedes albopictus* mosquito cells. Appl. Environ. Microbiol. 82, 3109–3120.

Moriyama, M., Nikoh, N., Hosokawa, T., Fukatsu, T., 2015. Riboflavin provisioning underlies *Wolbachia's* fitness contribution to its insect host. mBio 6 e01732-01715.

Noda, H., Koizumi, Y., Zhang, Q., Deng, K., 2001. Infection density of *Wolbachia* and

incompatibility level in two planthopper species, *Laodelphax striatellus* and *Sogatella furcifera*. Insect Biochem. Mol. Biol. 31, 727–737.
Riparbelli, M.G., Giordano, R., Callaini, G., 2007. Effects of *Wolbachia* on sperm maturation and architecture in *Drosophila simulans* Riverside. Mech. Dev. 124, 699–714.
Serbus, L.R., Casper-Lindley, C., Landmann, F., 2008. The genetics and cell biology of *Wolbachia*-host interactions. Annu. Rev. Genet. 42, 683–707.
Shropshire, D., On, J., Layton, E.M., Zhou, H., Bordenstein, S.R., 2018. One prophage WO gene rescues cytoplasmic incompatibility in *Drosophila melanogaster*. Proc. Natl. Acad. Sci. U.S.A. 115 (19) 201800650.
Simmons, L.W., Y-F, T., Millar, A.H., 2013. Sperm and seminal fluid proteomes of the field cricket *Teleogryllus oceanicus*: identification of novel proteins transferred to females at mating. Insect Mol. Biol. 22, 115–130.
Steve, D., Busby, S.A., Ursula, G., Jeffrey, S., Hunt, D.F., Karr, T.L., 2006. Genomic and functional evolution of the *Drosophila melanogaster* sperm proteome. Nat. Genet. 38, 1440–1445.
Subbarao, S.K., Curtis, C.F., Krishnamurthy, B.S., Adak, T.,., Chandrahas, R.K., 1977. Selection for partial compatibility with aged and previously mated males in *Culex pipiens* Fatigans (Diptera: culicidae). J. Med. Entomol. 14, 82–85.
Togo, T., Morisawa, M., 2004. GPI-anchored aminopeptidase is involved in the acrosome reaction in sperm of the *Mussel mytilusedulis*. Hum. Mol. Genet. 67, 465–471.
Tram, U., Sullivan, W., 2002. Role of delayed nuclear envelope breakdown and mitosis in *Wolbachia*-induced cytoplasmic incompatibility. Science 296, 1124–1126.
Wade, M.J., Chang, N.W., 1995. Increased male fertility in *Tribolium confusum* beetles after infection with the intracellular parasite *Wolbachia*. Nature 373, 72.
Wen, B., Zhou, R., Feng, Q., Wang, Q., Wang, J., Liu, S., 2014. Iquant: an automated pipeline for quantitative proteomics based upon isobaric tags. Proteomics 14, 2280–2285.
Werren, J.H., 1996. Biology of *Wolbachia*. Annu. Rev. Entomol. 42, 587–609.
Wu, M., Sun, L.V., Vamathevan, J., Riegler, M., Deboy, R., Brownlie, J.C., Mcgraw, E.A., Martin, W., Esser, C., Ahmadinejad, N., 2004. Phylogenomics of the reproductive parasite *Wolbachia* pipientis wMel: a streamlined genome overrun by mobile genetic elements. PLoS Biol. 2 e69.
Wu, C.M., Zong, Q., Du, A.L., Zhang, W., Yao, H.C., Yu, X.Q., Wang, Y.F., 2016. Knockdown of *Dynamitin* in testes significantly decreased male fertility in *Drosophila melanogaster*. Dev. Biol. 420, 79–89.
Xi, Z., Khoo, C.C.H., Dobson, S.L., 2005. *Wolbachia* establishment and invasion in an *Aedes aegypti* laboratory population. Science 310, 326–328.
Yasuhara, T., Yokosawa, H., Hoshi, M., Ishii, S., 1991. Involvement of a sperm aminopeptidase in fertilization of the sea urchin. Experientia 47, 100–103.
Yu, B., Li, D.T., Lu, J.B., Zhang, W.X., Zhang, C.X., 2016. Seminal fluid protein genes of the brown planthopper, *Nilaparvata lugens*. BMC Genomics 17, 654.
Yuan, L.L., Chen, X., Zong, Q., Zhao, T., Wang, J.L., Zheng, Y., Zhang, M., Wang, Z., Brownlie, J.C., Yang, F., Wang, Y.F., 2015. Quantitative proteomic analyses of molecular mechanisms associated with cytoplasmic incompatibility in *Drosophila melanogaster* induced by *Wolbachia*. J. Proteome Res. 14, 3835–3847.
Zhang, B., Chambers, M.C., Tabb, D.L., 2007. Proteomic parsimony through bipartite graph analysis improves accuracy and transparency. J. Proteome Res. 6, 3549–3557.
Zhang, K.J., Han, X., Hong, X.Y., 2013. Various infection status and molecular evidence for horizontal transmission and recombination of *Wolbachia* and *Cardinium* among rice planthoppers and related species. Insect Sci. 20, 329–344.
Zheng, Y., Ren, P.P., Wang, J.L., Wang, Y.F., 2011a. *Wolbachia*-induced cytoplasmic incompatibility is associated with decreased Hira expression in male *Drosophila*. PLoS One 6, e19512.
Zheng, Y., Wang, J.-L., Liu, C., Wang, C.-P., Walker, T., Wang, Y.-F., 2011b. Differentially expressed profiles in the larval testes of *Wolbachia* infected and uninfected *Drosophila*. BMC Genomics 12 595.
Zhu, J., Jiang, F., Wang, X., Yang, P., Bao, Y., Zhao, W., Wang, W., Lu, H., Wang, Q., Cui, N., 2017. Genome sequence of the small brown planthopper *Laodelphax striatellus*. GigaScience 6, 1–12.
Zug, R., Hammerstein, P., 2012. Still a host of hosts for *Wolbachia*: analysis of recent data suggests that 40% of terrestrial arthropod species are infected. PLoS One 7, e38544.